

Calculation of Inductance of Sparsely Wound Toroidal Coils

A. Pokryvailo

Spellman High Voltage Electronics Corp.

475 Wireless Blvd, Hauppauge NY 11788, apokryva@spellmanhv.com

Abstract: Analytical methods used widely for inductance calculation of toroidal coils yield large errors in the case of sparsely wound coils, especially when using low permeability cores. Numerical field calculations can provide “exact” figures. Being essentially 3D, such analysis is not straightforward. We have outlined several simulation methods. In this paper, we used AC/DC module in its “Magnetic Field” formulation. Simplifications, assumptions, and analysis bifurcations are described. In the model building, the first alternative is modeling full coil or using symmetry and thus modeling only part of the space. Both approaches were explored in this paper. Then, the winding was represented as a set of discrete toroidal turns, and then modeled as a toroidal helix. Both infinitely thin and finite thickness wires were modeled.

The main takeout from these simulations are physical aspects, which, if not revealed, were quantified, providing thus better insight into coils design and characterization.

Keywords: Comsol, toroidal coil, inductance, toroidal helix, symmetry.

1 Introduction

Usually the inductance of toroidal coils is calculated either analytically or empirically, on the base of the manufacturer-provided data. One common simplification in the first approach is calculating inductance of a long solenoid and “curving” the latter in a circular loop [1]. Core manufacturers usually specify inductance per turn L_1 , from which the coil inductance having W turns comes out as W^2L_1 . Both methods fall short in the case of sparsely wound coils, especially when using low permeability cores. Such coils are ubiquitous in high frequency inverters; sometimes, they are called “inverter chokes” (not to confuse with filtering chokes carrying mostly DC current).

Analytical inductance calculation of a *straight* helix is feasible [2], [3]. In principle, this may provide better understanding of the inductance dependence on the axial current components that

are tacitly neglected in common calculations [4], [5]. The inductance equations, however, are very complex, to the point of being unwieldable, to be of much use. In addition, extrapolations from straight helix to a real toroidal helix shape are risky.

Numerical field calculations, again in principle, can provide “exact” figures. Being essentially 3-D, such analyses are not straightforward. Below, we outline several possible modeling methods and systemize the obtained results.

2 Simplifications, assumptions and analysis bifurcations

Some assumptions that we made in the simulations are as follows.

1. For the simplicity sake, we neglect the coil leads. The latter can add quite a lot to the sparsely wound coil inductance, especially if a low-permeability core is used.
2. Winding is made by a round multistrand wire, the implication being that current density is constant throughout the wire cross-section. The turns are symmetrically spread on the core. We do not consider here windings with small number of turns wound densely on a small core area although such cases can be modeled within the limitations of the developed models.
3. For the simplicity sake, the toroidal core cross-section section is round, and the winding is a toroidal helix. The core is built as a torus primitive and is defined by its major radius $R_{core}=40$ mm and minor radius $r=10.5$ mm. This geometry approximates the Micrometals T400-2 core [6].
4. Core material is linear with constant permeability through its volume.

Relative permeability of the T400-2 core material is $\mu_{rel}=10$.

- In AC analyses, coil is excited by a sine wave.

In the model building, the first alternative is modeling full coil or using symmetry and thus modeling only $1/W$ of the space to minimize computing expense [7]. We model both options.

The winding can be represented as a set of W discrete toroidal turns or modeled as a toroidal helix. The next choice is accounting for or neglecting the wire thickness.

The above options will be clarified below.

3 Use of COMSOL Multiphysics

The problem was solved using the Magnetic Field interface. The governing subset of the Maxwell equations for the frequency domain is shown below:

$$(j\omega\sigma - \omega^2\epsilon_0\epsilon_r)\mathbf{A} + \nabla \times \mathbf{H} = \mathbf{J}_e$$

$$\mathbf{B} = \nabla \times \mathbf{A}$$

where ω is angular frequency, σ is material conductivity, ϵ_0 is permittivity of free space, ϵ_r is relative permittivity, \mathbf{A} is magnetic vector potential, \mathbf{H} is magnetic field, \mathbf{J}_e is current density, and \mathbf{B} is magnetic flux density. Although most of the problems were analyzed in the frequency domain, some cases were also solved in the steady-state approximation for a comparison with the frequency-domain solutions.

The model volume is limited by a sphere with a diameter of $4 \cdot R_{core}$, which is rather arbitrary. Such a confinement may be interpreted as having the inductor inside a metal chassis. If not mentioned otherwise, the wire radius $r_{wire}=2$ mm.

The materials used in the simulations are copper (wire material), ferrite (core), and air. Both air and ferrite are ascribed some low conductivity for better convergence.

Whenever possible, we used symmetry to decrease the model size. Periodic Boundary Condition (PBC) was employed for true symmetry emulation. Using other boundary conditions will be described further, specific to the analyzed cases.

4 Results

4.1 Discrete turns

A toroidal coil with a toroidal helix winding is shown in Figure 1a. One possible model simplification is representing the winding as a set of W discrete toroidal turns each carrying the same current. Then, from the symmetry considerations, the coil can be represented by a $1/W$ segment as shown in Figure 1b.

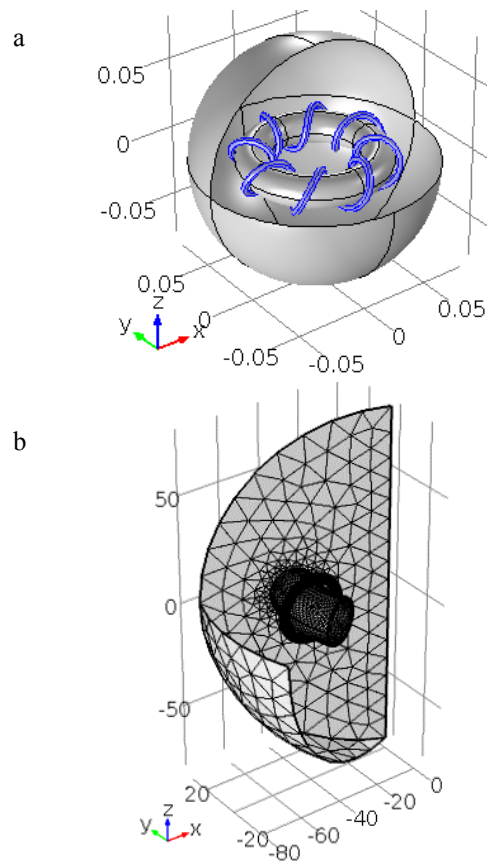


Figure 1. Model of a W -turn coil ($W=8$). Dimensions are in mm. Complete mesh consists of 121298 domain elements. Solution time is ~ 2 min per case on a PC with a 3.4 GHz CPU and 16 GB RAM.

Flux density B along the core midline is shown in Figure 2 for a number of W 's, and same for $W=8$ in the mid cross-section is shown in Figure 3. Note that B is strongly non-uniform along the core for low number of turns, which effectively invalidates the quadratic W^2

dependence of the coil inductance on number of turns. Table 1 gives the inductances, calculated and measured on core T400-2. The values denoted as “ L , H (calculated Micromet)” are the inductance of a single turn taken from [6] calculated to a W turns: $L=L_1 \cdot W^2$. Inductance measurements were done with a Quadtech LCR meter, model 1920, on a coil wound by a #18 AWG wire with leads ~ 5 cm. Note that the inductance measured at a low current may be drastically different from that measured at a high current, mostly, because of the core non-linearity. Table 2 giving the inductance dependence on the wire radius illustrates a known fact that thin wires have larger inductance than thick wires.

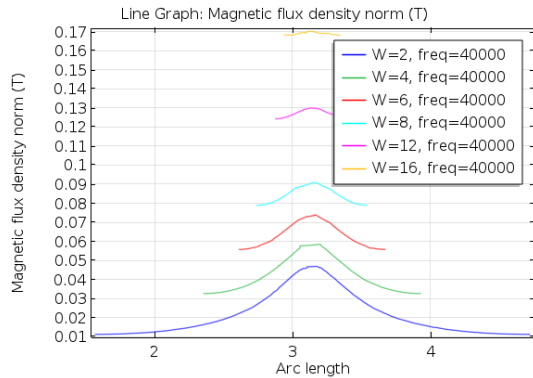


Figure 2. Flux density along core median line. Coil current is 150 Arms in all cases. Arc length (horizontal axis) is in radians.

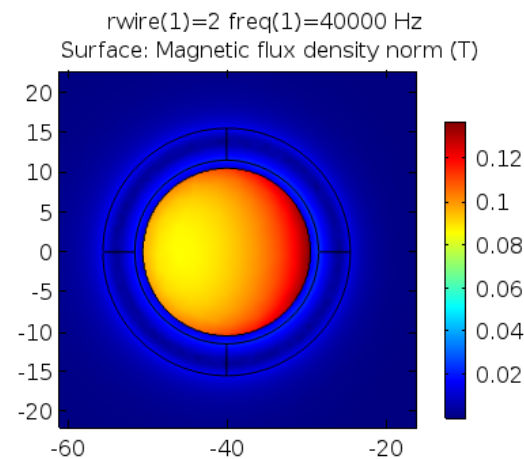


Figure 3. Flux density for 8 turns $W=8$ in mid cross-section.

Table 1. Inductances calculated and measured on core T400-2.

W	L , H discrete turns	L , H (calculated Micromet)	L , H measured
2	1.98E-07	7.20E-08	
4	4.75E-07	2.88E-07	1.00E-06
6	8.71E-07	6.48E-07	1.53E-06
8	1.40E-06	1.15E-06	2.20E-06
12	2.89E-06	2.59E-06	3.90E-06
16	4.96E-06	4.61E-06	

Table 2. Inductances calculated for discrete turns $W=8$ as function of wire radius. Edge Current excitation used for $rwire=0$.

$rwire$, mm	L , H (discrete turns)
0	2.1E-6
0.02	1.89E-06
0.05	1.82E-06
0.1	1.75E-06
0.2	1.67E-06
0.5	1.56E-06
1	1.48E-06
2	1.40E-06

4.2 Infinitely thin toroidal helix winding

Our model resembles closely that described in [7] and, probably, is built similarly. We model the helix as a parametric line, where parameter s sets how many turns would be modeled; $2\pi/W$ range corresponds to one full turn:

$$\begin{aligned} x: & (R_{core} + r_{hel} \cos(W*s)) * \cos(s) \\ y: & (R_{core} + r_{hel} \cos(W*s)) * \sin(s) \\ z: & r_{hel} \sin(W*s) \end{aligned}$$

where r_{hel} is the helix radius. In most simulations, $r_{hel}=r+2$ mm.

Figure 4 illustrates an example of such a model, and Figure 5 shows surface flux density induced by a 150 Arms current for full-space and $1/W$ section modeling. In the latter, we used PBC for true symmetry emulation. We note that

simulating discrete turns was done with a much friendlier Perfect Magnetic Conductor (PMC) boundary condition, which for that case was equivalent to PBC. Values of calculated inductance for both models are given in Table 3.

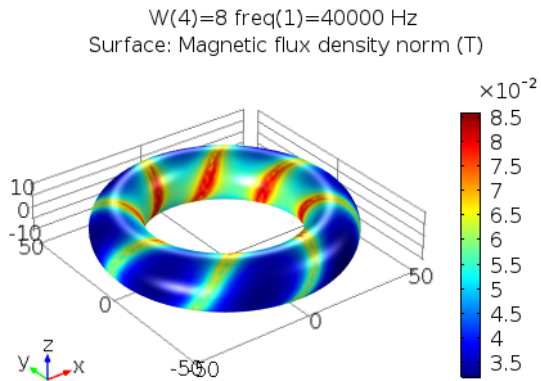


Figure 4. Toroidal helix $W=8$ winding (full space modeled) represented by a single filament 2 mm apart from core (approximating 4 mm wire wound closely to core).

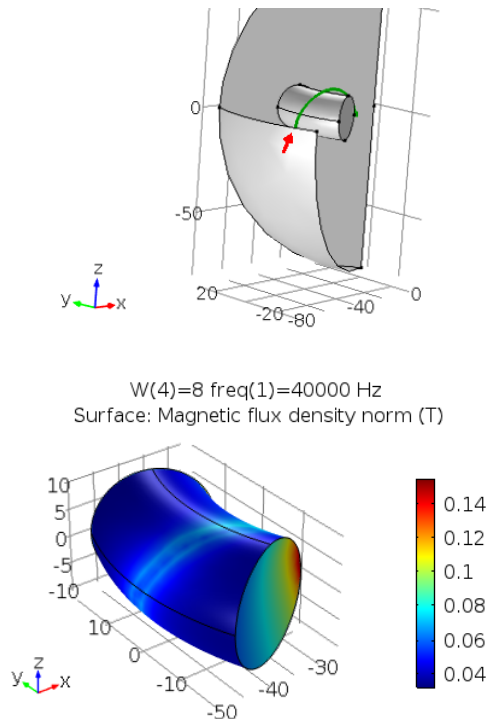


Figure 5. Toroidal helix $W=8$ winding (one turn) represented by a single filament 2 mm apart from core (approximating 4 mm wire wound closely to core).

Table 3. Toroidal helix (edge current) inductance for l/W and full space model.

W	L, H	
	one turn	full
2	4.79E-07	4.76E-07
4	7.84E-07	7.81E-07
6	1.20E-06	1.24E-06
8	1.74E-06	1.83E-06
12	3.16E-06	3.45E-06
16	5.04E-06	5.65E-06

4.3 Full coil model

Up to now, we have simulated the coil wire in two approximations: a – “full-bodied” but non-helical, straightened wire (discrete turns), and b – helical, but infinitely thin wire. We could not find a ready expression for a parametrized toroidal helix surface. Rather, we built the wire by sweeping a circle along the toroidal helix. The first attempt was exploiting symmetry to reduce the problem size. This failed when applying PBC, although simulations with PMC ran through smoothly. Thus, we performed full-size model simulations with the same parameters as before; some field plots are shown in Figure 6.

Table 4 shows that the wire thickness has more pronounced impact on the inductance value than in the discrete-turns simulations. Such difference is explained by much longer wire length compared to discrete turns. Note that inductance of an infinitely thin wire is infinity.

Table 5 gives inductance calculated for the full volume model for different number of turns and different core permeabilities, μ_{rel} . The wire radius was 2 mm in these simulations. It is also illustrative of the dominance of the wire inductance in sparse winding, especially with a low-permeability core. An alternative statement would be that a large part of magnetic field energy is stored outside the core (e.g., 73% for $W=2$, $\mu_{rel}=10$). Indeed, comparing the extremes of $W=2$ for $\mu_{rel}=1, 100$, we see a difference of the inductance of only 5.1 times, and not 100. There is also no quadratic dependence on number of turns at low permeability. However, at $\mu_{rel}>100$, such dependence is observed.

Determining fringe field (it depends on the coil build and its environment) is an important capability of numerical simulations for the considered cases. Knowledge of fringe field is essential in choice of materials that could be heated by eddy currents, EMC considerations, etc. This can also help in the choice of the coil type:

cylindrical, e.g., a Brooks coil for the maximum inductance [4], [5], or a larger toroidal coil for low fringe field (see more on the subject in [8]). Figure 7 shows an example of fringe field for the coil with $W=8$, $r_{wire}=2$ mm on the coil z-axis and in the core median plane.

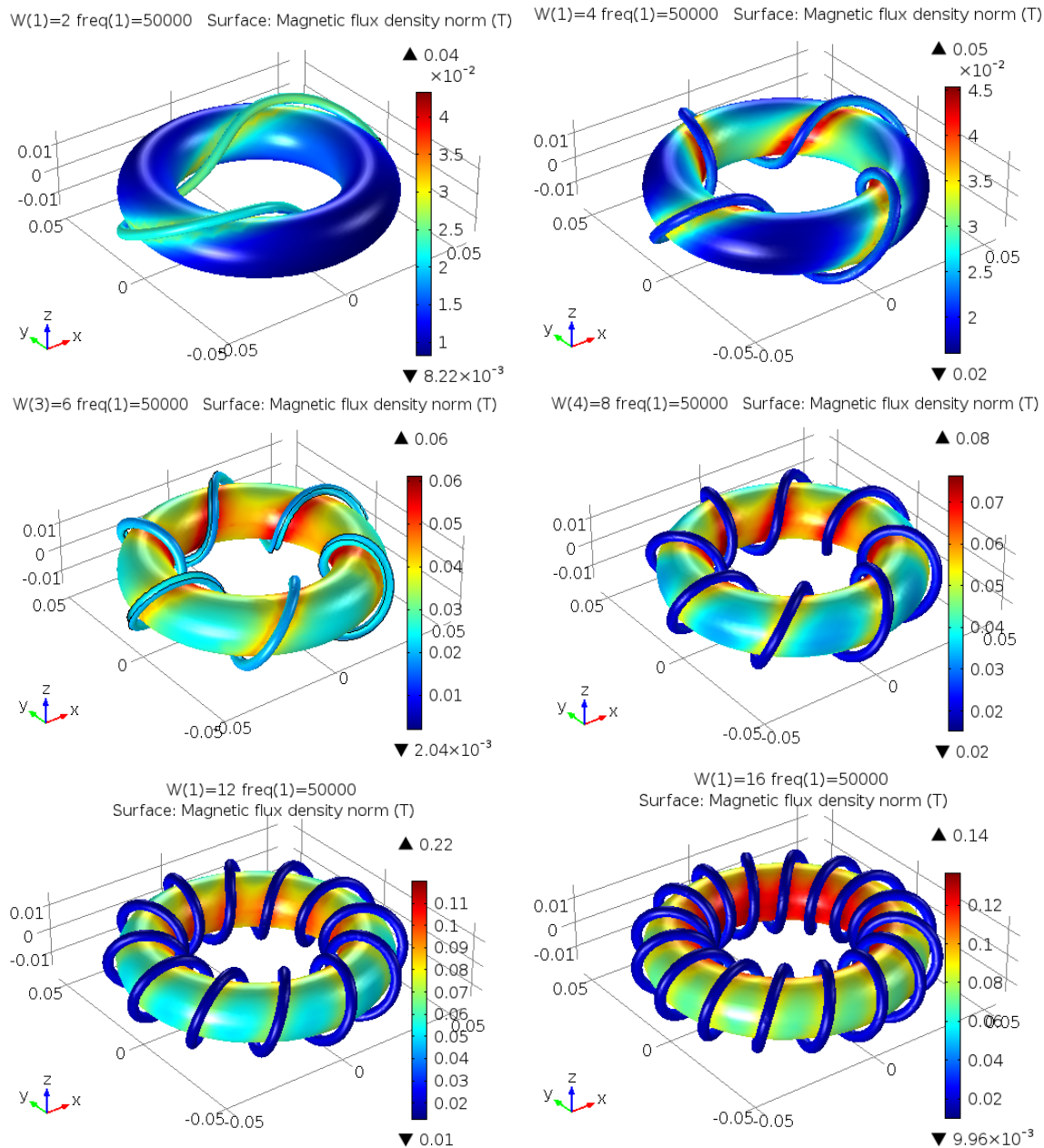
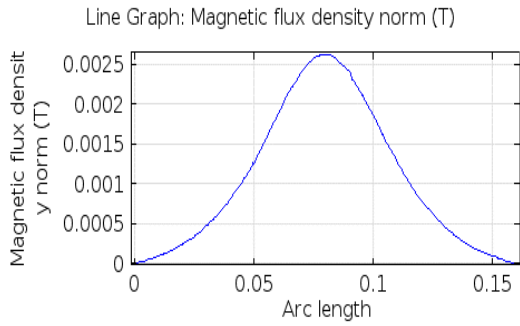
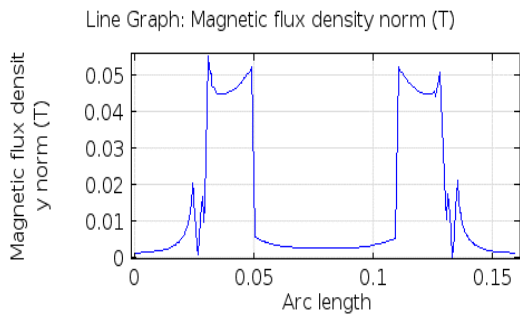


Figure 6. Flux density for $W=2, 4, 6, 8, 12, 16$. Winding current is 150 Arms for all cases. $\mu_{rel}=10$, $r_{wire}=2$ mm. Mesh consists of 139189 domain elements ($W=8$). Solution time is ~ 1.5 min per case.



a



b

Figure 7. Field on core axes for $W=8$. a – along z , b – along x .

Table 4. Inductance calculated in full volume model, $W=4$, as function of wire radius.

r_{wire} , m	L , H
1.00E-04	1.68E-06
2.00E-04	1.50E-06
5.00E-04	7.28E-07
0.001	6.20E-07
0.002	5.36E-07

Table 5. Inductance, H, calculated in full volume model for different number of turns, and different core permeabilities, μ_{rel} . Wire radius $r_{wire}=2$ mm.

W	$\mu_{rel}=1$	$\mu_{rel}=10$	$\mu_{rel}=100$
2	1.94E-07	2.97E-07	9.89E-07
4	2.42E-07	5.46E-07	3.17E-06
6	3.22E-07	9.31E-07	6.99E-06
8	3.94E-07	1.50E-06	1.16E-05
12	6.38E-07	3.01E-06	2.64E-05
16	9.51E-07	5.14E-06	4.67E-05

4.4 Comparison of inductance calculated by different methods

Table 6 summarizes calculations described in the previous sections. A couple of comments are in order.

Table 6. Comparison of coils inductance, H, calculated by different methods. “Helix” refers to infinitely thin, or filament, wire modeled as edge current. In discrete turns and full wire models, $r_{wire}=2$ mm if not stated otherwise.

W	Discrete turns DC, 1/W model	Helix, 1/W model, PBC, DC	Helix, 1/W model, PBC, 40 kHz	Full helix model, 40 kHz	Full helix model, DC	Full wire model 50 kHz	Full wire model DC	Calculated from Micromet	Measured
2	1.98E-07	4.77E-07	4.79E-07	4.76E-07	4.76E-07	2.97E-07	2.97E-07	7.20E-08	
4	4.75E-07	7.83E-07	7.84E-07	7.81E-07	7.81E-07	5.46E-07	5.44E-07	2.88E-07	1.00E-06
6	8.71E-07	1.24E-06	1.20E-06	1.24E-06	1.24E-06	9.31E-07	9.30E-07	6.48E-07	1.53E-06
8	1.40E-06	1.84E-06	1.74E-06	1.83E-06	1.83E-06	1.50E-06	1.46E-06	1.15E-06	2.20E-06
12	2.89E-06	3.46E-06	3.16E-06	3.45E-06	3.45E-06	3.01E-06	2.94E-06	2.59E-06	3.90E-06
16	4.96E-06	5.66E-06	5.04E-06	5.65E-06	5.65E-06	5.14E-06	5.01E-06	4.61E-06	

1. Some frequency-domain simulations were made at 40 kHz, other at 50 kHz. The frequencies are cited for documentary purpose only, because the results are virtually indistinguishable.
2. Comparing frequency-domain and stationary solutions, we see that they are identical for the partial size, $1/W$, discrete turns model with PMC used, and for the infinitely thin full helix models. There is a slight difference between the solutions for the full wire and partial size, $1/W$, models with filament current and PBC used. Since no eddy currents are involved, one would expect no difference between DC and AC cases. Moreover, the inductances calculated from the stationary solutions are the same for the partial and full models. We do not have explanation to that, but, intuitively, full models seem to be more consistent.
3. The catalog values are not far off both the simulation and measurement results at $W \geq 8$. At a lower number of turns, the error becomes an order of magnitude.
4. Whereas a toroidal helix is relatively simple to model, modeling a real winding on a core having a rectangular cross-section is not so simple. On the other hand, it is seen that the simplest discrete-turns model is adequate for $W \geq 6$, which implies that the same technique can be used for inductance calculation of the above type of coils.

5 Conclusions

Some physical aspects, if not revealed but quantified in the simulations, are quite useful. They are as follows:

1. For sparsely wound coils, the dependence of the inductance on number of turns is far from being quadratic;
2. As a corollary, for low-permeability cores, wire inductance is a considerable factor, especially for very low number of turns and large-diameter, small cross-section area cores;
3. Fringe field of a coil sparsely wound on a low-permeability core is low but not negligible.

From the modeling perspective, we note that:

1. Using a discrete-turns approximation results in a large error when modeling a sparsely wound coil;
2. Fringe field can be calculated reducing the winding to an edge current. However, inductance calculation had better be done with a finite wire thickness.

6 References

- [1] A.V. Bossche and V.C. Valchev, "Inductors and Transformers for Power Electronics", CRC Press, Boca Raton, 2005. P. 8.1.3
- [2] C. Snow, "Formula for the Inductance of a Helix Made with Wire of Any Section", Scientific Papers of the Bureau of Standards, Vol. 21, Scientific Paper 537 (S537), 1926, p. 431-519.
- [3] C. Snow, "A Simplified Precision Formula for the Inductance of a Helix with Corrections for the Lead-In Wires", NBS Journal of Research Vol. 9, RP479, June 1932.
- [4] F.W. Grover, "Inductance Calculations", D. Van Nostrand, 1946; Reprint: Dover, 2004.
- [5] P. L. Kalantarov and L. A. Zeitlin, "Inductance Calculation", 3rd Ed., Leningrad, EnergoAtomIzdat, 1986 (in Russian), 488pp.
- [6] "Micrometals Iron Powder Cores", Catalog, Issue L, February 2007.
- [7] W. Frei, "Exploiting Symmetry to Simplify Magnetic Field Modeling", Comsol blog, 2014. Available at <https://www.comsol.com/blogs/exploiting-symmetry-simplify-magnetic-field-modeling/>
- [8] M. Kanter, A. Pokryvailo, N. Shaked, and Z. Kaplan, "Factors in Inductive Storage System Design", Proc. 10th Pulsed Power Conf., Albuquerque, July 10-13, 1995, pp. 186-191.

7 Acknowledgements

The author thanks Spellman High Voltage Electronics Corp. for supporting this work.